


Article

Efficient Synthesis of Furfural from Corncob by a Novel Biochar-Based Heterogeneous Chemocatalyst in Choline Chloride: Maleic Acid–Water

Linsong Yang ^{1,†}, Yucheng Li ^{1,†}, Yuqi Wu ^{1,†}, Yucai He ^{1,2,*}  and Cuiluan Ma ³

¹ School of Pharmacy, Changzhou University, Changzhou 213164, China; linsongyang@cczu.edu.cn (L.Y.); s21091055082@smail.cczu.edu.cn (Y.L.); wyq12@163.com (Y.W.)

² State Key Laboratory of Bioreactor Engineering, School of Biochemical Engineering, East China University of Science and Technology, Shanghai 200237, China

³ State Key Laboratory of Biocatalysis and Enzyme Engineering, School of Life Sciences, Hubei University, Wuhan 430062, China; macuiluan@163.com

* Correspondence: yucaihe@cczu.edu.cn or heyuca2001@163.com

† These authors contributed equally to this work.

Abstract: The use of plentiful and renewable feedstock for producing chemicals is fundamental for the development of sustainable chemical processes. Using fish scale as a biobased carrier, a novel biochar $\text{SO}_4^{2-}/\text{SnO}_2$ -FFS heterogeneous chemocatalyst was prepared to catalyze furfural production from xylose-rich corn cob-hydrolysates obtained from acid hydrolysis of corn cob in a deep eutectic solvent (DES)–water system. By characterizing the physical as well as chemical properties of $\text{SO}_4^{2-}/\text{SnO}_2$ -FFS by NH_3 -TPD, FT-IR, XPS, XRD, and SEM, it was shown that the chemocatalyst had Lewis/Brønsted acid centers, and its surface roughness could be well expanded to contact substrates. The corn cob was initially hydrolyzed at 140 °C to obtain xylose-rich hydrolysate. Subsequently, $\text{SO}_4^{2-}/\text{SnO}_2$ -FFS (3.6 wt.%) was used to catalyze the corn cob hydrolysate containing *D*-xylose (20.0 g/L) at a reaction temperature of 170 °C for 15 min. Additionally, ZnCl_2 (20.0 g/L) was added. Ultimately, furfural (93.8 mM, 70.5% yield) was produced in the deep eutectic solvent ChCl:maleic acid–water ($\text{DES}_{\text{MLA}}\text{-water} = 10:90, v/v$). A synergistic catalytic mechanism for transforming xylose-rich corn cob-hydrolysate into furfural and byproducts were proposed using $\text{SO}_4^{2-}/\text{SnO}_2$ -FFS as a chemocatalyst in $\text{DES}_{\text{MLA}}\text{-water}$ containing ZnCl_2 . Consequently, the efficient use of biochar $\text{SO}_4^{2-}/\text{SnO}_2$ -FFS chemocatalysts for the sustainable synthesis of biobased furan compounds from biomass holds great promise in the future.

Keywords: biofuran; biochar catalyst; deep eutectic solvent; ZnCl_2 ; lignocellulose



Citation: Yang, L.; Li, Y.; Wu, Y.; He, Y.; Ma, C. Efficient Synthesis of Furfural from Corncob by a Novel Biochar-Based Heterogeneous Chemocatalyst in Choline Chloride: Maleic Acid–Water. *Catalysts* **2023**, *13*, 1277. <https://doi.org/10.3390/catal13091277>

Academic Editors: Anand Kumar, Siham Y. Al-Qaradawi and Mohamed Ali S. Saad

Received: 23 July 2023

Revised: 27 August 2023

Accepted: 30 August 2023

Published: 5 September 2023



Copyright: © 2023 by the authors. Licensee MDPI, Basel, Switzerland. This article is an open access article distributed under the terms and conditions of the Creative Commons Attribution (CC BY) license (<https://creativecommons.org/licenses/by/4.0/>).

1. Introduction

The continued use of non-renewable energy has raised people's awareness of natural resource depletion and global warming, shifting the focus of many countries to renewable energy [1,2]. It is known that lignocellulosic biomass (LB) is renewable and eco-friendly [3–5], which is considered a replacement for manufacture biofuels, materials, and high-value biobased compounds because it is plentiful, inexpensive, and promising [6–10]. As one of the important chemical intermediates, furfural (FAL) can be transformed from lignocellulose or its derivatives (e.g., xylan and *D*-xylose) via hydrothermal reaction [11]. In industrial production, FAL has been widely used. It has become a raw material for pharmaceuticals, industrial solvents, and numerous fuel additives [12]. By deeper processing, it can be transformed into various furan-based compounds (e.g., tetrahydrofuran, furoic acid, tetrahydrofuran, dihydropyran, acetyl furan, furfuryl alcohol, and furfurylamine) [13].

Generally, furfural (FAL) can be synthesized using both homogeneous and heterogeneous catalysts. Utilizing homogeneous catalysts such as hydrochloric acid, the highest

FAL yield from xylose could reach 37.5% [14]. Combining Lewis acid (AlCl_3) and Brønsted acid (HCl) as homogeneous catalysts for the catalytic conversion of untreated cellulose resulted in a remarkable FAL yield of 75% [15]. However, the use of homogeneous catalysis might accelerate equipment corrosion and lead to difficulties in recycling, posing challenges in terms of both economic efficiency and environmental sustainability [16]. Consequently, more eco-friendly heterogeneous catalysts have been employed for FAL synthesis [17,18]. Among these, sulfonated carbon derived from biomass has garnered attention due to its low cost, favorable thermal stability, and acidity. Using biochar-based $\text{SO}_4^{2-}/\text{SnO}_2\text{-CS}$ as a catalyst, the corn stalk was transformed into FAL with a yield of 68% at a temperature of 170 °C for 0.5 h [19]. A total of 62% of FAL yield from *D*-xylose by carbonized and sulfonated teff straw was achieved in a toluene-water system at 170 °C for 0.5 h [20]. FAL was synthesized from corncob with sulfonated tin-loaded rice husk-activated carbon, and the yield of FAL was 40.9% [21]. Employing 4-BDS as a sulfonating agent, sucrose was carbonized into a solid acid catalyst, achieving a 61% FAL yield from a corn stalk in 100 min at a temperature of 200 °C [22]. This highlights the significant potential of using biomass as a catalyst carrier. Therefore, utilizing sulfonated carbon derived from biomass as a catalyst or carrier is essential for achieving high-value utilization of biomass.

Appropriate solvents also play a crucial role in enhancing FAL productivity [23]. Deep eutectic solvents (DESs) are defined as systems that combine eutectic Lewis (L) or Brønsted (B) acids with various ionic species [24]. Compared to traditional reaction systems, DESs offer several advantages including ease of preparation, non-toxicity, non-volatility, and reusability [25]. Utilizing choline chloride (ChCl)-lactic acid as a chemical catalyst and reaction medium, rice straw was transformed into FAL (12% yield) at 180 °C for 2 h [26]. Water-ChCl:oxalic acid was employed as a medium to convert corncob (CC) at 180 °C for 0.5 h, achieving a FAL yield of 46% [27]. ChCl-carboxylic acid containing H^+ and Cl^- might facilitate the dehydration of *D*-xylose to produce FAL [28]. Therefore, to further enhance the FAL yield, a synergistic catalysis approach using carboxylic acid-based DES and heterogeneous catalysts can be employed in the reaction system, providing a more environmentally friendly and efficient means of catalyzing biomass-derived *D*-xylose into FAL.

As one kind of bioresource, fish scales are rich in collagen, hydroxyapatite (HAP), and lipids [29]. According to the statistics, the fish processing industry produces about 30 million tons of fish waste each year, which contains 4% of fish scales. In recent years, fish scales have been used in the chemistry, medicine, and food industry [30]. As one main component of fish scales, HAP is a calcium phosphate biomaterial, which serves as an ideal catalyst carrier due to its ion exchange, adsorption, acid–base properties, and stability. Currently, there is limited information on the effective transformation of biomass or *D*-xylose to FAL using fish scale-based biochar solid acid catalysts. In order to realize the reuse of fresh fish scales (FFS) and improve the efficiency of FAL production by biomass catalysis, a novel biochar heterogeneous catalyst ($\text{SO}_4^{2-}/\text{SnO}_2\text{-FFS}$) was prepared using FFS as a carrier. The structure and morphology of $\text{SO}_4^{2-}/\text{SnO}_2\text{-FFS}$ were characterized by $\text{NH}_3\text{-TPD}$, FT-IR, XPS, XRD, and SEM. In addition, an attempt was made to synthesize FAL from hydrolysate from CC in DES_{MLA} -water system using $\text{SO}_4^{2-}/\text{SnO}_2\text{-FFS}$ as a heterogeneous catalyst. The process conditions for preparing FAL (such as $\text{SO}_4^{2-}/\text{SnO}_2\text{-FFS}$ dosage, catalytic temperature, catalytic time, cycle time, chloride salt, etc.) were optimized. Finally, a sustainable strategy for the synthesis of FAL using fish scale-based heterogeneous catalysts in an environmentally friendly catalytic reaction system was established (Figure 1)

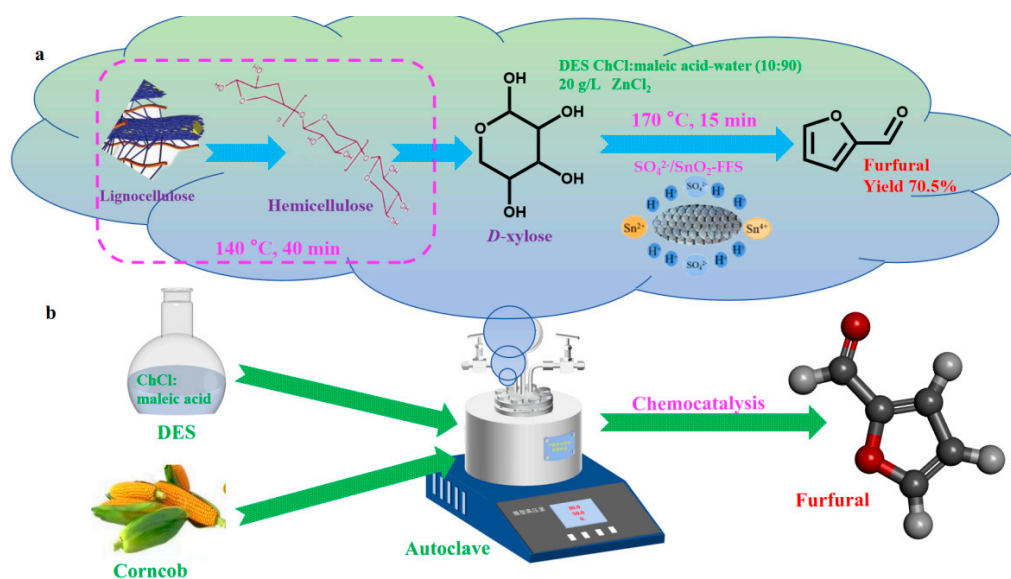


Figure 1. The process of catalytically converting the *D*-xylose solution obtained from the hydrolysis of corncob at 140 °C for 40 min into FAL using $\text{SO}_4^{2-}/\text{SnO}_2$ -FFS in a DES-water system (a); a chemical strategy for synthesis of FAL from corncob with biochar-based heterogeneous chemocatalyst (b).

2. Results and Discussion

2.1. Characterization of Biochar-Based Catalyst $\text{SO}_4^{2-}/\text{SnO}_2$ -FFS Using FFS as Biobased Carrier

FFS of carp is one of the underutilized fishery wastes [31]. Tin-based heterogeneous chemocatalysts have been proven to be able to utilize to dehydrate corncob-derived *D*-xylose to FAL. In this work, sulfonated tin-loaded heterogeneous chemocatalyst $\text{SO}_4^{2-}/\text{SnO}_2$ -FFS was prepared by using carbonized FFS as biobased carrier. The surface area changes of $\text{SO}_4^{2-}/\text{SnO}_2$ -FFS and FFS were tested by BET, and the results were displayed in Table 1. The surface change of the carrier FFS and catalyst $\text{SO}_4^{2-}/\text{SnO}_2$ -FFS was compared. Specific surface area (SSA) of FFS was 12.4 m^2/g . $\text{SO}_4^{2-}/\text{SnO}_2$ -FFS had bigger SSA (29.4 m^2/g). Large SSA might promote the contact between the catalytic active sites on solid acid catalyst and the substrate molecules, which would result in the enhancement of FAL productivity [32]. $\text{SO}_4^{2-}/\text{SnO}_2$ -FFS appeared smaller pore size (4.7 nm) compared with the FFS pore size (14.5 nm), and a reduced pore volume of $\text{SO}_4^{2-}/\text{SnO}_2$ -FFS (0.010 cm^3/g) was evident. The pore size of $\text{SO}_4^{2-}/\text{SnO}_2$ -FFS was bigger than the molecular dynamics (MD) radius of FAL (0.68 nm) and *D*-xylose (0.86 nm) [33], suggesting that *D*-xylose might be beneficial to spread into the acid sites on the surface of $\text{SO}_4^{2-}/\text{SnO}_2$ -FFS and was further dehydrated into FAL.

Table 1. Surface and pore difference of FFS and $\text{SO}_4^{2-}/\text{SnO}_2$ -FFS.

Sample	BET Surface Area, m^2/g	Pore Volume, cm^3/g	Pore Size, nm
FFS	12.4	0.03	14.5
$\text{SO}_4^{2-}/\text{SnO}_2$ -FFS	29.4	0.01	4.7

The SEM image depicted that the surface of FFS was comparatively smooth, while the surface of $\text{SO}_4^{2-}/\text{SnO}_2$ -FFS was rough (Figure 2). It showed that SnO_2 and SO_4^{2-} were loaded on the carrier FFS, and enhanced the contact between $\text{SO}_4^{2-}/\text{SnO}_2$ -FFS and *D*-xylose. As described in FT-IR (Figure 3), $\text{SO}_4^{2-}/\text{SnO}_2$ -FFS had obvious surface compared to FFS. The peaks near 3421 cm^{-1} and 2922 cm^{-1} were attributed to the presence of hydroxyl groups and H^+ of -COOH stretching [34]. The peak about 1628 cm^{-1} corresponded to the stretching vibration of the amide in FFS [35]. The peak around 1404 cm^{-1} was associated with O-H stretching [36]. The peak near 1128 cm^{-1} corresponded to sulfonic acid groups

(SO₃H) [37]. The peaks around 741 cm⁻¹ and 592 cm⁻¹ were related to the inorganic phase, representing the bending mode of P-O groups, as well as hydroxyl stretching of the adsorption water [38]. The XRD spectra of FFS and SO₄²⁻/SnO₂-FFS were displayed in Figure 4. The peak near 26.1° was associated with the crystal plane of amorphous carbon [39], and the peak around 31.9° was assigned to hydroxyl apatite [40]. The sharp characteristic peaks of crystalline SnO₂ were reflected at 25.9°, 33.8°, and 51.9° through the XRD analysis [41]. The observed XRD pattern was characteristic for HAP as reported in the literature [42]. XRD patterns of SO₄²⁻/SnO₂-FFS also indicated that SnO₂ had been loaded. By using NH₃-TPD (temperature-programmed desorption of ammonia) (Figure 5), the acid properties of SO₄²⁻/SnO₂-FFS were measured. Through the analysis with desorption of NH₃ under the various temperatures, the weak-, medium-, and strong-acid sites on the heterogeneous catalyst might be detected based on the temperature 100–200 °C, 200–400 °C, and 400–800 °C, respectively. From the observation of Figure 5, it could be deduced that SO₄²⁻/SnO₂-FFS possessed a predominant type of acid site (weak acid site) only at 108 °C. As displayed in XPS image (Figure 6), SO₄²⁻/SnO₂-FFS had been accompanied by Sn, and Sn had three valences (+4, +2, 0). The fraction of Sn⁴⁺3d_{5/2}, Sn²⁺3d_{5/2}, and Sn⁰3d_{5/2} were 48.4%, 46.1%, and 5.5%, respectively.

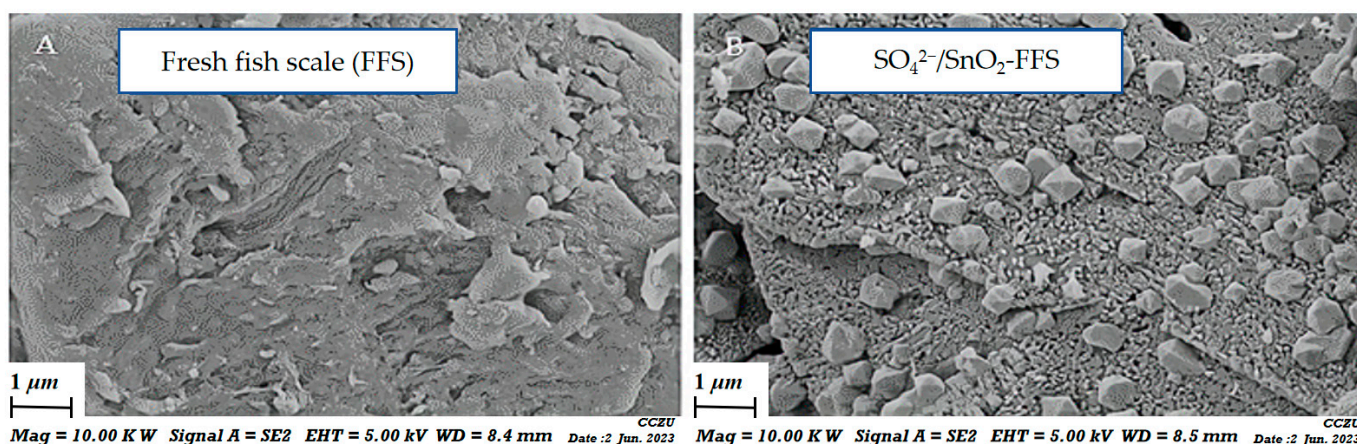


Figure 2. SEM image of FFS (A) and solid acid SO₄²⁻/SnO₂-FFS (B).

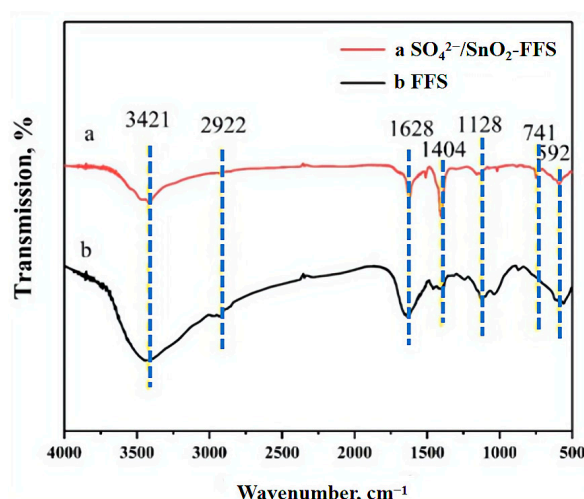


Figure 3. Fourier transform infrared spectroscopy (FT-IR) images of chemocatalyst SO₄²⁻/SnO₂-FFS and FFS. FT-IR was conducted by using Nicolet IS50 (Thermo Scientific, Waltham, MA, USA) in the range of 4000–500 cm⁻¹.

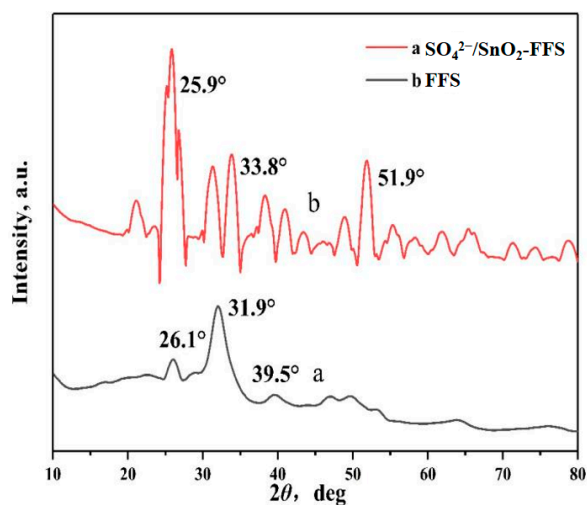


Figure 4. X-ray diffraction (XRD) images of chemocatalyst $\text{SO}_4^{2-}/\text{SnO}_2\text{-FFS}$ and FFS (XRD was carried out by using a D/max-2500 (Japan) instrument (Rigaku Co., Akishima-shi, Japan)). The 2θ angle was scanned between 10° and 80° .

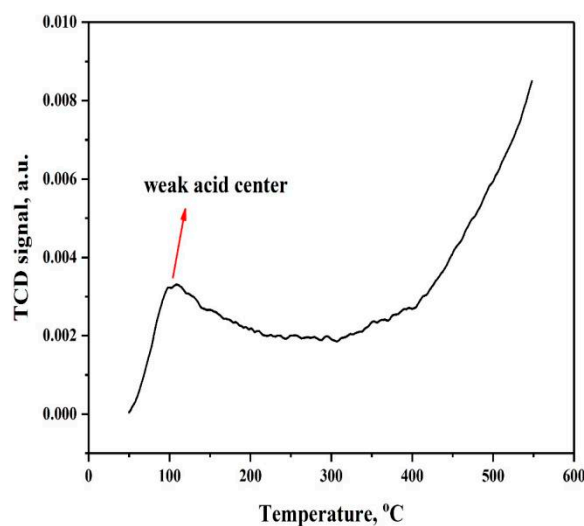


Figure 5. Temperature-programmed desorption of ammonia ($\text{NH}_3\text{-TPD}$) image of $\text{SO}_4^{2-}/\text{SnO}_2\text{-FFS}$. The temperature was scanned between $0\text{--}600^\circ\text{C}$.

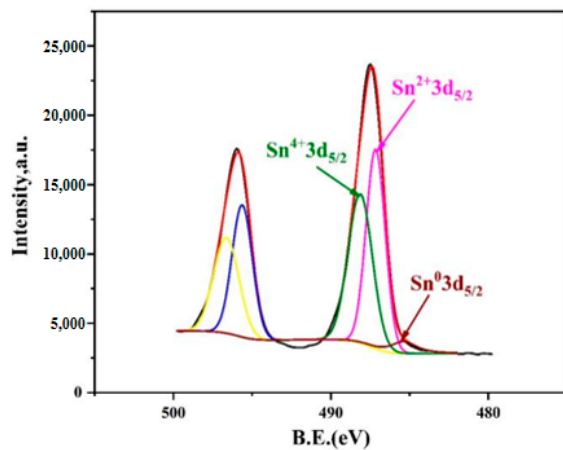


Figure 6. X-ray photoelectron spectroscopy (XPS) image of $\text{SO}_4^{2-}/\text{SnO}_2\text{-FFS}$. The B.E. (eV) was scanned between $480\text{--}500$.

It has been reported that tin and sulfonic acid group have good catalytic activity for FAL production, forming lignocellulose and xylose-rich hydrolysate [43]. By comparing the surface structure, pore properties, and chemical groups, $\text{SO}_4^{2-}/\text{SnO}_2$ -FFS preparation process could slightly alter the surface structure of FFS. The preparation of $\text{SO}_4^{2-}/\text{SnO}_2$ -FFS involved the solvent immersion and sulfonation reaction by H_2SO_4 , which would result in the dissolution of FFS and the disordered structure. Sn^{4+} as the Lewis acid center on the tin-based solid acid could promote the production of FAL [19].

2.2. Effects of $\text{SO}_4^{2-}/\text{SnO}_2$ -FFS Load, Dehydration Temperature, and Reaction Duration on the FAL Generation

To promote the generation of FAL, three key parameters including $\text{SO}_4^{2-}/\text{SnO}_2$ -FFS load (0–4.8 wt.%), dehydration temperature (160–190 °C), and reaction duration (10–50 min) were tested on the dehydration of xylose. As displayed in Figure 7a, when the loading of $\text{SO}_4^{2-}/\text{SnO}_2$ -FFS increased from 0 to 3.6 wt.%, a significant enhancement in FAL yield was observed, and a maximum (48.8% yield) was obtained in the existence of 3.6 wt.% $\text{SO}_4^{2-}/\text{SnO}_2$ -FFS at 160 °C in 15 min. With increasing the $\text{SO}_4^{2-}/\text{SnO}_2$ -FFS content from 3.6 to 4.8 wt.%, the FAL yields did not change apparently. Significantly, the suitable load of $\text{SO}_4^{2-}/\text{SnO}_2$ -FFS was 3.6 wt.%. Sulfonated montmorillonite (2.0 wt.%) transformed corncob to FAL (40% yield) under the temperature of 180 °C after 10 min [44]. Sulfonated argil (3.6 wt.%) transformed *D*-xylose (20 g/L) to FAL (44% yield) after 20 min under the temperature of 180 °C [45]. In this work, $\text{SO}_4^{2-}/\text{SnO}_2$ -FFS (3.6 wt.%) catalyzed corncob hydrolysates containing *D*-xylose under the temperature of 160 °C after 15 min to generate FAL in the yield of 48.8% yield.

By comparing the yield of reaction at 160–190 °C for 10–50 min, the highest FAL yield (58.8%) was achieved at 170 °C for 15 min, and the reaction temperature was higher compared with the optimization measures in the previous step. When the dehydration temperature was above 170 °C, the dehydration activity was weakened, achieving a declined FAL yield. A higher performance temperature did not favor the formation of FAL [46], and a low FAL yield could be obtained [47]. Although a higher dehydration temperature might increase the dehydration activity for converting xylose into FAL, the unwanted side-reaction potentially would happen [48]. Some unnecessary substances might deposit in the catalytic centers on $\text{SO}_4^{2-}/\text{SnO}_2$ -FFS, and significant influence the catalytic activity and the FAL yield was thusly decreased [19]. When the reaction duration was more than 15 min, the generation of FAL was weakened (Figure 7b). $\text{SO}_4^{2-}/\text{SnO}_2$ -FFS had good catalytic activity to catalyze the synthesis of FAL from corncob-derived *D*-xylose within 15 min at 170 °C.

In order to analyze the impact of the $\text{SO}_4^{2-}/\text{SnO}_2$ -FFS catalyst on FAL yield, xylose aqueous solution was employed as the substrate in a DES_{MLA} -water system, with the addition of ZnCl_2 , and the reaction was conducted at 170 °C for 15 min. The results are presented in Table S1 (in Support Information), revealing that SnO_2 -FFS and $\text{SO}_4^{2-}/\text{SnO}_2$ could give higher FAL yields compared to the control group without a catalyst. Furthermore, the FAL was achieved in the highest yield (70.5%) through the catalysis of $\text{SO}_4^{2-}/\text{SnO}_2$ -FFS. This could be attributed to the synergistic effect of Lewis and Brønsted acidic sites in sulfonated SnO_2 -FFS, resulting in more active acid sites [49,50]. In summary, the solid acid catalyst $\text{SO}_4^{2-}/\text{SnO}_2$ -FFS employed in this study exhibited enhanced catalytic activity in biomass conversion to FAL.

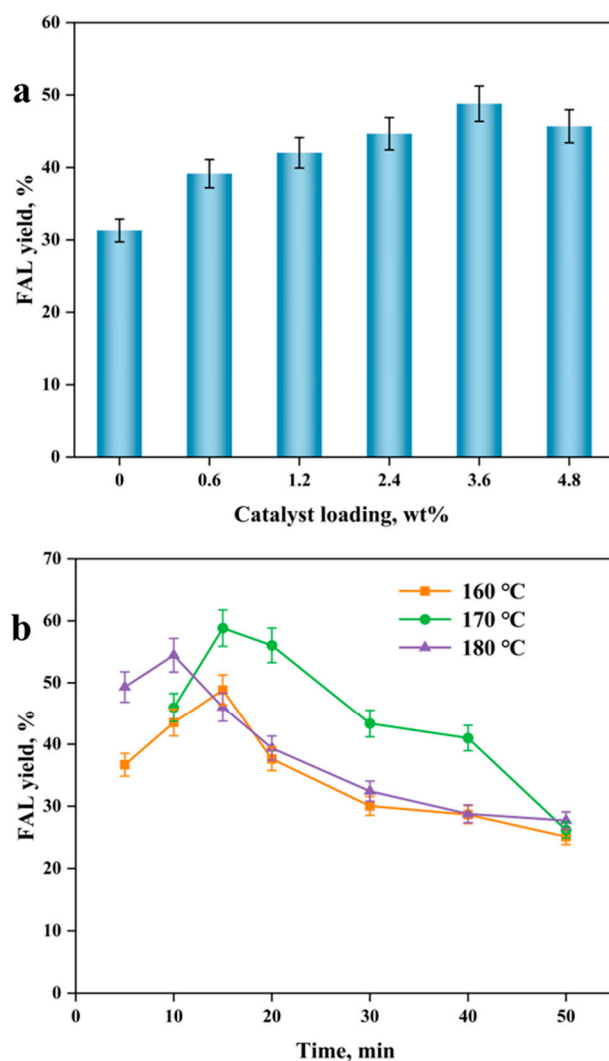


Figure 7. Effects of catalyst $\text{SO}_4^{2-}/\text{SnO}_2\text{-FFS}$ loading (0–4.8 wt.%) on the FAL yield (xylose-rich hydrolysate containing 20 g/L xylose, 0–4.8 wt.% $\text{SO}_4^{2-}/\text{SnO}_2\text{-FFS}$, 160 °C, 15 min, 500 rpm) (a); effects of reaction temperature (160–180 °C) and duration (5–50 min) on the FAL yield (xylose-rich hydrolysate containing 20 g/L xylose, 3.6 wt.% $\text{SO}_4^{2-}/\text{SnO}_2\text{-FFS}$, 500 rpm) (b).

2.3. Effects of DES–Water Systems on the FAL Formation

DES acted as a reaction solvent in the catalytic transformation of lignocellulose and its derived sugars [51,52]. Five kinds of carboxylic acids, including maleic acid (MLA) (pKa = 1.9), malic acid (MA) (pKa = 3.46), lactic acid (LA) (pKa = 3.86), citric acid (CA) (pKa = 3.13), and tartaric acid (TA) (pKa = 3.04), were selected to synthesize DESs (DES_{MLA} , DES_{MA} , DES_{LA} , DES_{CA} , and DES_{TA}) with ChCl (hydrogen bond acceptor, HBA). Using 3.6 wt.% $\text{SO}_4^{2-}/\text{SnO}_2\text{-FFS}$ as a catalyst, xylose-rich hydrolysates were catalyzed to generate FAL in a DES–water (20:80, *v/v*) system. The dissociation constant (pKa) values of carboxylic acids in DESs were close to those in water and also might be associated with the FAL yield [53]. When xylose was dehydrated into FAL in acidic DESs, the pKa value of carboxylic acid in DESs had a certain correlation with the yield of FAL. The results indicated that a lower pKa value would give a higher the yield of FAL (Figure 8a). The carboxylic acid with low pKa value in DES was beneficial to the FAL generation. As a hydrogen bond donor (HBD), MLA has the lowest pKa value (1.9), which facilitated to the FAL formation (FAL yield 63.0%). The dicarboxylic structure of MLA with stable positive anions might form by hydrogen bonds due to the action of protonation. The cis-anion structure could bind to ChCl to enhance the generation of a more stable liquid, which was necessary for transforming *D*-xylose efficiently into FAL. Additionally, with the increase in the -OH

group in the carbon chain, the pKa value of carboxylic acid in DESs would be lower and a higher FAL yield would be obtained [54]. Using MLA (pKa = 1.9), CA (pKa = 3.13) and LA (pKa = 3.86) as HBDs, the prepared ChCl-based DESs had apparently influenced the FAL yields. In the water system, the yield of FAL was 58.8%, which was lower than the yield of FAL in DES_{MLA}-water (63.0% yield). The influence of the DES_{MLA}-H₂O volumetric ratio (0:1–4:6, *v/v*) was examined on the FAL generation through the conversion of *D*-xylose-rich corn-cob-hydrolysate into FAL with SO₄²⁻/SnO₂-FFS (Figure 8b). In the DES_{MLA}-water system, the FAL yield exhibited a significant increase with the rising volumetric ratio of DES_{MLA}. When DES was absent from the reaction system, the FAL yield approached 60%. However, with an increase in DES_{MLA} volumetric ratio up to 10%, the yield of FAL exceeded 60%. The highest yield was achieved in DES_{MLA}-water (1:9, *v/v*). Furthermore, as the volumetric ratio of DES_{MLA} was further increased, the FAL yield displayed a noticeable decline. A high content of DES_{MLA} (> 10%) would increase the viscosity of the reaction medium, leading to the reduction in FAL yield. Accordingly, DES_{MLA}-water (1:9, *v/v*) was regarded as the most suitable reaction system.

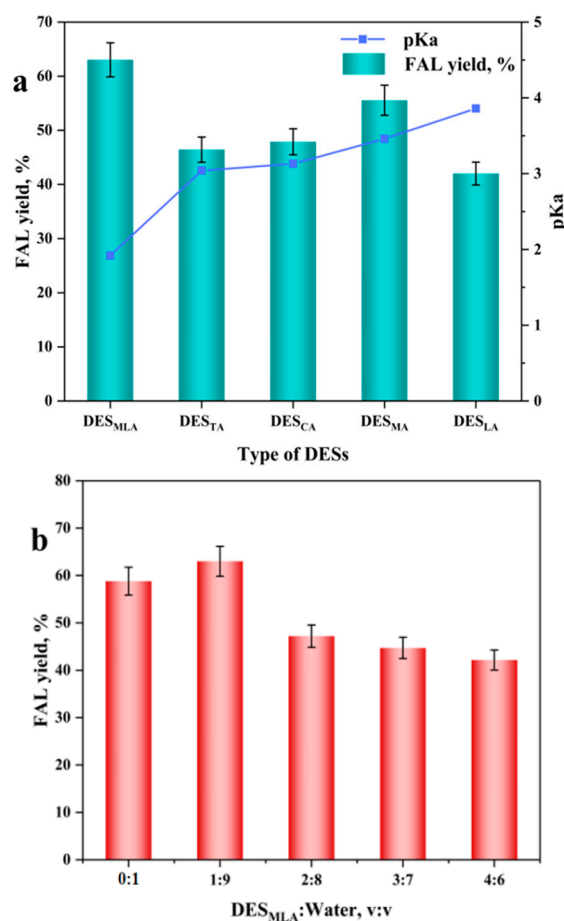


Figure 8. Effect of different DES type and the pKa value of different organic acid in DES on the FAL yield in DES-water (20:80, *v/v*) system (xylose-rich hydrolysate containing 20 g/L xylose, 3.6 wt.% SO₄²⁻/SnO₂-FFS, 170 °C, 15 min, 500 rpm) (a); effect of DES_{MLA}-water system (0:1–7:3, *v/v*) on the FAL yield (xylose-rich hydrolysate containing 20 g/L xylose, 3.6 wt.% SO₄²⁻/SnO₂-FFS, 170 °C, 15 min, 500 rpm) (b).

2.4. Effect of Chloride Salts on the FAL Yield

Chloride salts are frequently employed to stabilize the transition state and intermediate structures in catalytic processes, thereby reducing undesirable side reactions and significantly improving the yield of FAL [55]. Hence, different chloride salts (15 g/L) were individually supplemented into the catalytic system, which would result in the promotion

of the dispersion and yield of FAL. Distinct from the control group, SnCl_4 and LiCl could apparently hinder the production of FAL (Figure 9a). Most of the chloride salts (CaCl_2 , MgCl_2 , NH_4Cl , AlCl_3 , KCl , MnCl_2 , BaCl_2 , and NaCl) did not significantly promote the catalytic activity. However, NiCl_2 and ZnCl_2 exhibited positive effects on the enhancement of catalytic reactions. Particularly, the addition of ZnCl_2 (15 g/L) facilitated the FAL formation and resulted in the highest FAL yield of 66.6%. Moreover, different loads of ZnCl_2 (0–30 g/L) were supplemented into DES_{MLA} -water mediums (Figure 9b), and the catalytic effect on the generation of FAL from *D*-xylose was tested. When the content of ZnCl_2 was 20 g/L, the highest FAL yield reached 70.5% for 15 min in DES_{MLA} -water (170 °C). In the absence of ZnCl_2 , the FAL yield was only 63%. The addition of ZnCl_2 enhanced the selectivity of FAL production from xylan-rich biomass, reducing the occurrence of side reactions and the formation of by-products [56]. As a result, this led to a further increase in the overall FAL yield.

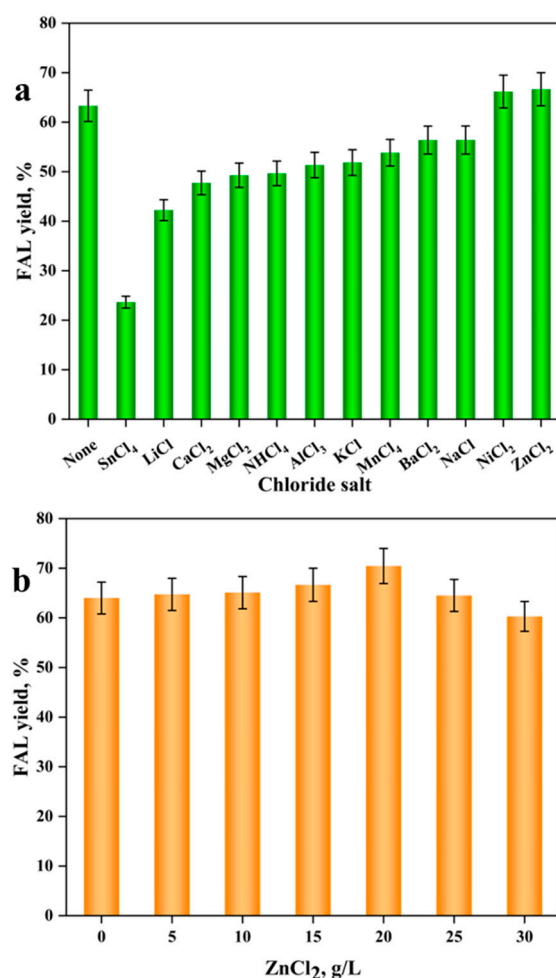


Figure 9. Effect of different chloride salts (15 g/L) on the FAL yield (xylose-rich hydrolysate containing 20 g/L xylose, 3.6 wt.% SO_4^{2-} /SnO₂-FFS, DES_{MLA} -water system (1:9, *v/v*), 170 °C, 15 min, 500 rpm) (a); effect of ZnCl_2 dosage (0–30 g/L) on the FAL yield (xylose-rich hydrolysate containing 20 g/L xylose, 3.6 wt.% SO_4^{2-} /SnO₂-FFS, DES_{MLA} -water system (1:9, *v/v*), 170 °C, 15 min, 500 rpm) (b).

To sum up, the yield of FAL was up to 70.5% from *D*-xylose-rich corncob-hydrolysate (20 g/L) by 3.6 wt.% SO_4^{2-} /SnO₂-FFS and 20 g/L ZnCl_2 in DES_{MLA} -water (1:9, *v/v*) system. Various solid acids prepared by different carriers were used to catalyze the synthesis of FAL from biomass or xylose. Using Sn-adamellite or Sn-sepiolite as a catalyst, biomass treated by an alkalic solution was catalyzed into FAL under acidic conditions, and the yields

were below 60% [57]. Sn-zeolite, $\text{SO}_4^{2-}/\text{SnO}_2\text{-CS}$, and Sn-GP were also employed to transform lignocellulose to FAL in the yield of 52.3%, 68.2%, and 47.3%, respectively [16,19,29]. Coconut shell-activated carbon-based biochar solid acid transformed sugarcane bagasse to FAL with a yield of 49% [11]. Accordingly, $\text{SO}_4^{2-}/\text{SnO}_2\text{-FFS}$ had high catalytic ability for the catalysis of biomass to yield FAL (70.5% yield). Notably, this was the first report that fish scale-based solid acids could be efficiently utilized to catalyze biomass into FAL with high yield in $\text{DES}_{\text{MLA}}\text{-water}$.

2.5. Recyclability of $\text{SO}_4^{2-}/\text{SnO}_2\text{-FFS}$ and $\text{DES}_{\text{MLA}}\text{-Water}$

The main benefit of using solid acid catalysts is that they can be easy to recycle and reuse [58]. In order to test the stability of $\text{SO}_4^{2-}/\text{SnO}_2\text{-FFS}$ used in *D*-xylose dehydration to prepare FAL in $\text{DES}_{\text{MLA}}\text{-water}$, a five-cycle experiment was carried out. Before each use, the recovered catalyst was regenerated by sulfonation. As displayed in Figure 10, FAL could reach 70.5% by using fresh $\text{SO}_4^{2-}/\text{SnO}_2\text{-FFS}$. Then, the yield of FAL dropped to 66.6% at 170 °C for 15 min in the $\text{DES}_{\text{MLA}}\text{-water}$ system at the first reuse of the catalyst, and the FAL yield was weakened gradually to 54.2% after five cycles. The catalytic ability of $\text{SO}_4^{2-}/\text{SnO}_2\text{-FFS}$ decreased slightly but it still could achieve a yield of FAL up to 54%, which had a favorable thermostability. Furthermore, the reduction in catalytic ability might be related to the loss of the catalytic component SnO_2 . Sn-zeolite was reused seven times, and the FAL yields were declined from 52% (1st batch) to 37% (seventh batch) [16]. After three cycles of Sn-MMT, the yield of FAL was weakened by 12% [59]. These results displayed that $\text{SO}_4^{2-}/\text{SnO}_2\text{-FFS}$ had good reusability and high thermostability. The good reusability of $\text{SO}_4^{2-}/\text{SnO}_2\text{-FFS}$ could effectively reduce operating costs. Furthermore, DES_{MLA} also could be reused. After being extracted and purified, $\text{DES}_{\text{MLA}}\text{-water}$ was recycled for the next batch. It could be reused five times without a remarkable impact on the productivity of FAL. In conclusion, well recyclability and stability of $\text{DES}_{\text{MLA}}\text{-water}$ showed high potential for industrial production of FAL.

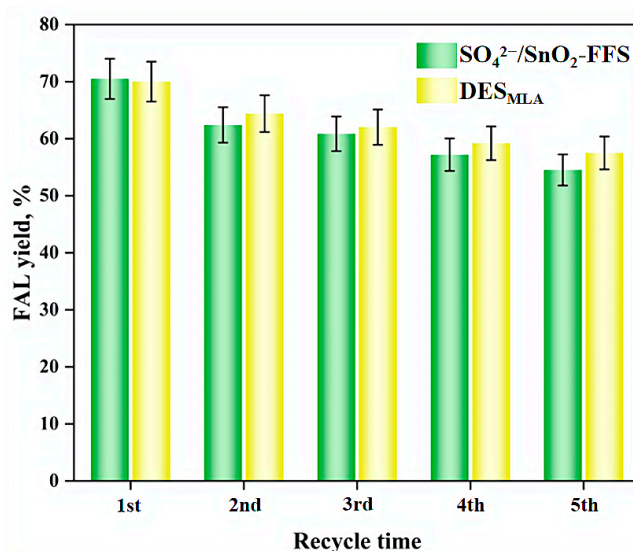


Figure 10. Recycled of $\text{SO}_4^{2-}/\text{SnO}_2\text{-FFS}$ and DES_{MLA} catalyzed xylose-rich hydrolysate to FAL (xylose-rich hydrolysate containing 20 g/L xylose, 3.6 wt.% $\text{SO}_4^{2-}/\text{SnO}_2\text{-FFS}$, $\text{DES}_{\text{MLA}}\text{-water}$ system (1:9, *v/v*), 20 g/L ZnCl_2 , 170 °C, 15 min, 500 rpm).

2.6. Mass Flow from Corncob to FAL

In Figure 11, the mass flow from CC to FAL in $\text{DES}_{\text{MLA}}\text{-water}$ system was summarized. The 100 g of CC consisted of 41.5 g of glucan, 31.5 g of xylan, 22.5 g of lignin and 4.5 g of others. 1 L of *D*-xylose hydrolysate (containing 20 g *D*-xylose) was obtained after acidolysis of 100 g CC. After carbonization, sulfonation, and loading on FFS, $\text{SO}_4^{2-}/\text{SnO}_2\text{-FFS}$ was finally obtained. The FAL preparation was generally carried out in a 10 L stainless steel

reactor which contained 20 g of *D*-xylose, 36 g of catalyst, 0.1 L DES_{MLA} , 0.9 L water and 20 g ZnCl_2 , then the reaction was well-distributed and mixed at 170 °C for 15 min by stirring at 500 rpm. In the DES_{MLA} -water system, 20 g of *D*-xylose was converted into 9.0 g of FAL. The yield of FAL reached up to 70.5%. This result of mass balance confirmed that CC could be utilized to produce FAL effectively via $\text{SO}_4^{2-}/\text{SnO}_2$ -FFS. In the fish processing industry, 1 million tons of fish scale are produced each year [60]. Fish scale is an economic, abundant, and sustainable bioresource. In this study, the carbonized fish scale was utilized as a carrier to synthesize biochar-based heterogeneous $\text{SO}_4^{2-}/\text{SnO}_2$ -FFS catalyst for producing FAL via the dehydration of *D*-xylose in a sustainable reaction system (DES_{MLA} -water). The waste FFSs were prepared into biochar-based solid acid and catalyzed to produce FAL, which realized the efficient utilization of FFSs. A core-shell sulfonated tin-loaded diatomite catalyst could be utilized to prepare FAL from xylose with a yield of 66% [61]. $\text{SO}_4^{2-}/\text{SnO}_2$ -FFS, which was produced by utilizing carbonized FFS as a carrier, transformed xylose-rich hydrolysate to FAL with a yield of 70.5% at 170 °C for 15 min in DES_{MLA} -water. Apparently, the abundant and renewable fish scale could be utilized to prepare solid acid for the catalytic synthesis of FAL from biomass hydrolysates efficiently.

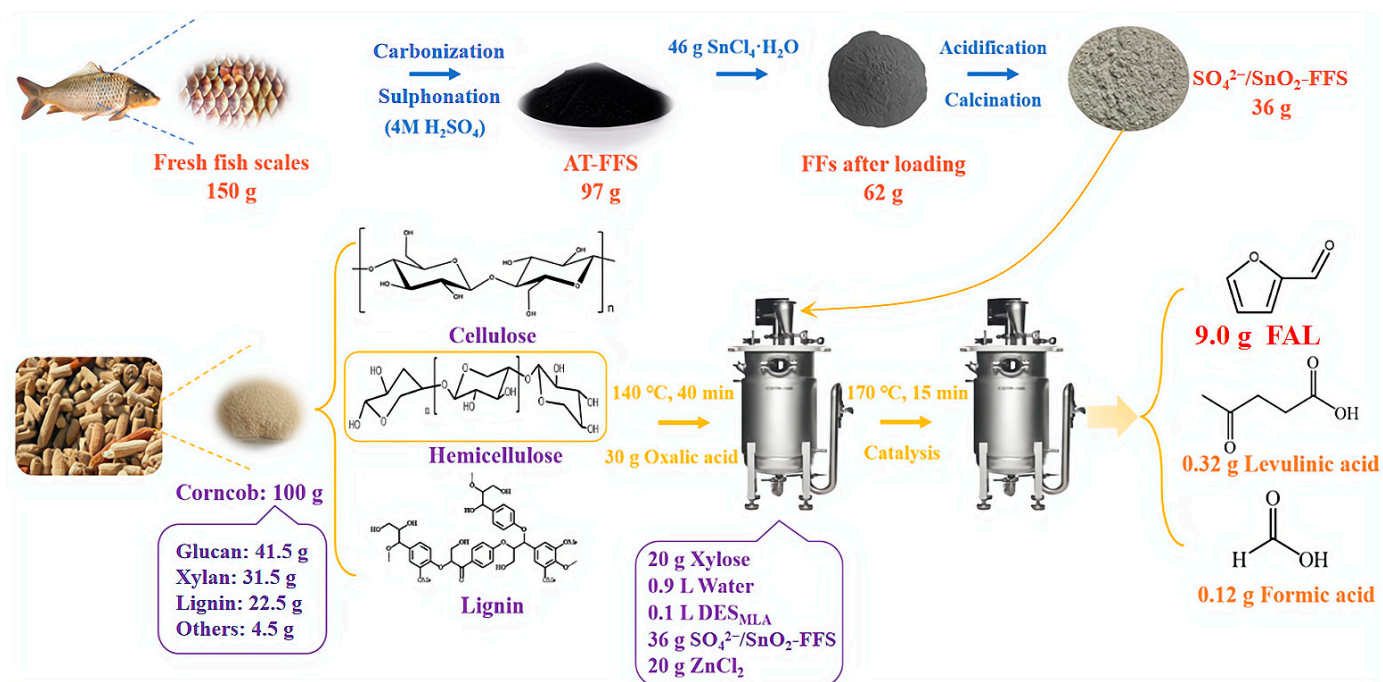


Figure 11. Mass flow for corncob (CC) to FAL.

2.7. Proposed Mechanism for Synergistic Catalysis of *D*-Xylose-Rich Hydrolysate into FAL in DES_{MLA} -Water

In this study, the biochar catalyst $\text{SO}_4^{2-}/\text{SnO}_2$ -FFS is a biomass-based carbon material with a pore size of 4.5 nm (Table 1), high surface area, and contained uniform load content (Figure 1). In the $\text{SO}_4^{2-}/\text{SnO}_2$ -FFS catalyst, the induction effect of S=O might cause the electron cloud on the Sn-O to deviate wildly, which would strengthen the L acid site [62]. The hydroxyl group (-OH) of HAP in FFSs might be replaced by fluoride, chloride, and carbonate ions to form fluoroapatite or chloroapatite. The Ca^{2+} can be replaced with various metal ions through an ion exchange reaction to generate apatite corresponding to metal ions. Sn ions had been successfully loaded into $\text{SO}_4^{2-}/\text{SnO}_2$ -FFS, which might have a positive effect on the catalytic efficiency of FAL [63]. Furthermore, the L acid site on $\text{SO}_4^{2-}/\text{SnO}_2$ -FFS had a strong attraction to the electrons of water molecules, which could dissociate the L acid site and then form the B acid site. In the dehydration reaction,

DES_{MLA} could be utilized as both catalyst and solvent with acidic and ionic properties to transform biomass-derived sugars to FAL.

In an aqueous system, it was speculated that SO₄²⁻/SnO₂-FFS and DES_{MLA} had a synergistic catalytic action in the production of FAL (Figure 12). According to the HPLC analysis results, the reaction solution contained *D*-xylose, glucose, cellobiose, formic acid, levulinic acid, and FAL (data not shown). Sn ions and acid ions were uniformly supported on the catalyst carrier. The proposed catalytic mechanism was as follows: the loop-opening reaction of *D*-xylose from *D*-xylose hydrolysate of CC produced chain structure, and the L acid site of SO₄²⁻/SnO₂-FFS cooperated with acyclic *D*-xylose to generate more reactive isomer through hydrogen transfer reaction. FAL was further synthesized by loop-closing and dehydration by B acid. The pore size of the FFS carbon base was suitable for contact between *D*-xylose and the active center, which might promote the transformation of *D*-xylose. Moreover, the HAP component in FFS was prone to ion exchange reactions with tin ions, and tin ions had a certain attraction to sulfate ions and chloride ions, which improved the acidity. ChCl might improve the proton availability and activity in the system under acidic conditions. Additionally, Cl⁻ from ChCl could be beneficial to the isomerization of the *D*-xylose molecule and strengthen its attraction on the SO₄²⁻ site, which might increase the reaction rate [64]. It was worth noting that chloride salt might accelerate the transformation of *D*-xylose from lignocellulose to FAL [65]. Hence, DES_{MLA} played a synergistic role in FAL production when SO₄²⁻/SnO₂-FFS was used as a chemocatalyst. In addition, under this system, glucose from hydrolysate might be isomerized and dehydrated to form HMF, which could be also partially decomposed into formic acid and levulinic acid.

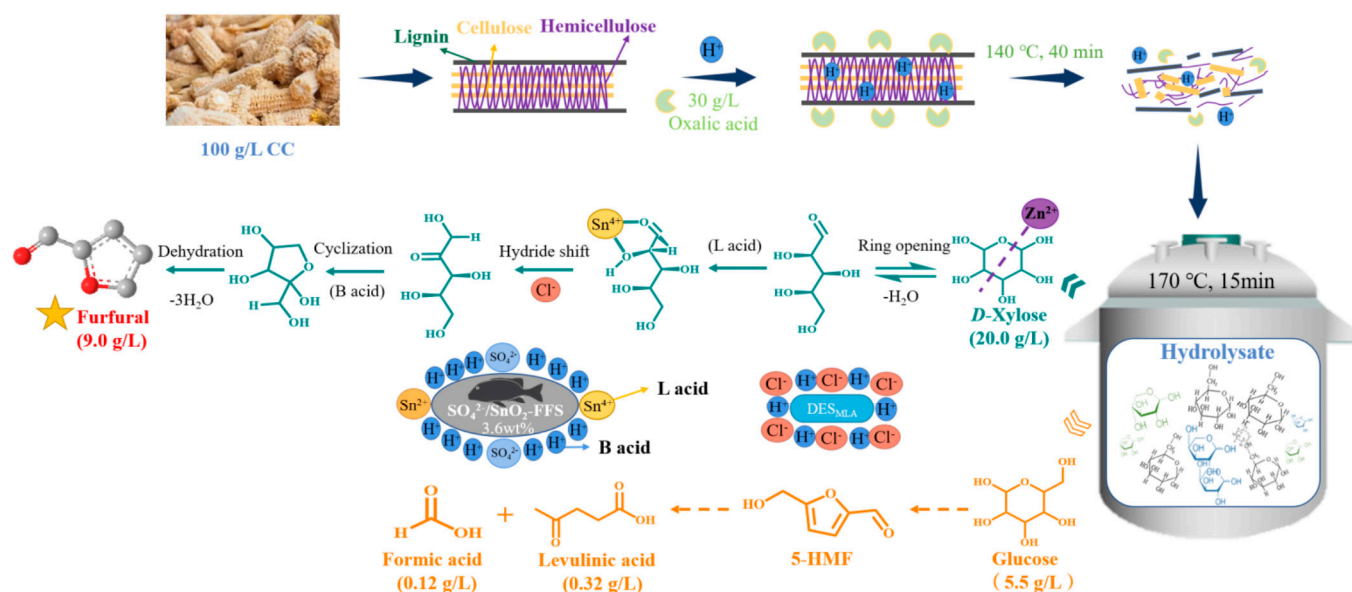


Figure 12. Proposed catalytic mechanism for catalyzing *D*-Xylose hydrolysate of CC into FAL and byproduct at 170 °C for 15 min with 20 g/L ZnCl₂ in DES_{MLA}–water (1:9, *v/v*) system.

Clean production of biobased chemicals from renewable lignocellulose is essential in a sustainable biorefinery [66]. Lignocellulose, with its wide range of sources, low cost, and sustainable production, can be derived from various biomass materials (e.g., straw, bagasse, wheat husk, etc.) for the production of FAL [67]. In China, about 900 million tons of crop waste are produced each year, 11.1% of which is CC [65]. In addition, FFS as a waste bioresource has good biocompatibility and degradability, and excellent mechanical properties due to their highly ordered layered microstructure and composition similar to human hard tissue, which has been utilized in tissue engineering, biological filling, sewage processing, and flexible electronics [30]. In this study, FFS was first used as a carrier to prepare biochar chemocatalyst (SO₄²⁻/SnO₂-FFS) for FAL production. The yield of

FAL (70.5%) was obtained by catalyzing the CC-hydrolysate containing xylose to FAL in DES_{MLA}-water system using SO₄²⁻/SnO₂-FFS as catalyst, verifying that available, cheap, and renewable FFS could be used as a bio-based carrier for the synthesis of highly catalytic activity of heterogeneous biochar catalysts to transform biomass-derived *D*-xylose into FAL in a high yield. Compared with the conditions or yields of FAL production from biomass or xylose catalyzed by other solid acids, the yield of FAL by SO₄²⁻/SnO₂-FFS was higher, the reaction time was shorter, and the reaction solution could be reused, which would not only save energy, but also be more friendly to the environment. Apparently, the prepared biochar catalyst catalyzed biomass for FAL production has full application prospects.

3. Materials and Methods

3.1. Reagents and Materials

Fresh fish scale of carp was collected from a fishery in Weifang (Weifang, China). Choline chloride (ChCl), malic acid (MA), maleic acid (MLA), lactic acid (LA), Citric acid (CA), tartaric acid (TA), MgCl₂, NaCl, KCl, FeCl₃, AlCl₃, CrCl₃, CuCl₂, CoCl₂, NH₄Cl, ZnCl₂, furfural (FAL), SnCl₄·5H₂O, ammonia, ethanol, sulfuric acid (H₂SO₄), and other chemicals were bought from other commercial sources (Shanghai, China).

3.2. Synthesis of DESs

DES was prepared according to the procedure as previously reported [68]. The seven DESs used in this study were DES_{LA}, DES_{MA}, DES_{CA}, DES_{MLA}, and DES_{TA}. These DESs were prepared by mixing ChCl and a corresponding organic acid at 80 °C. The ratio of ChCl to organic acid was 1:1 (mol/mol).

3.3. Preparation of Xylose-Rich Hydrolysate from Corncob and SO₄²⁻/SnO₂-FFS Catalyst

Xylose-rich hydrolysate from corncob was produced by hydrothermal reaction. Corncob was hydrolyzed with DES_{MLA} at 140 °C for 40 min. Then, xylose-rich hydrolysate was obtained by filtration. By concentration, the xylose in hydrolysate reached 20 g/L.

FFS was thoroughly washed with tap water, followed by boiling in deionized water. Subsequently, the boiled mixture was filtered to remove gelatin, proteins, and other impurities. The obtained wet fish scale was then dried in a 60 °C oven for 16 h. The desiccated solid was finely ground using a milling machine to achieve particle sizes between 60 and 80 mesh. Finally, the powdered fish scale was placed in a muffle furnace and subjected to a temperature of 300 °C for 1 h, resulting in the formation of biochar. The obtained powders were immersed in 4 M H₂SO₄ at 60 °C for 4 h for sulfonation. The sulfonated solid powders were obtained by filtration and rinsed continuously with deionized water until neutral. The acid-treated FFS (AT-FFS) was blended with SnCl₄·5H₂O and anhydrous ethanol, and then ammonia (25.0 wt.%) was slowly dripped into this mixture to regulate the pH to 6.0. This generated colloidal liquor was dried in an oven (70 °C) for 12 h and then oven dried at 90 °C for another 12 h. The collected powders were steeped in 500 mM H₂SO₄ for 180 min. The acidic solid powders were separated by filtration. The powders were dried for 12 h in an oven (80 °C), and then calcined in a muffle furnace (500 °C) for 4 h. Finally, the formed SO₄²⁻/SnO₂-FFS was collected for further use.

3.4. Transformation of Xylose-Rich Hydrolysate into FAL by SO₄²⁻/SnO₂-FFS in DES-Water System

In 40 mL DES-water system, xylose-rich hydrolysate (20 g/L) was mixed with SO₄²⁻/SnO₂-FFS in a 100 mL stainless-steel autoclave (TGYP-A-0.1L, Zhengzhou Huate Instrument Equipment Co., Ltd., Zhengzhou, China) by stirring (500 rpm). After the xylose-rich corncob-hydrolysate was catalyzed with SO₄²⁻/SnO₂-FFS (0–4.8 wt.%) at 160–180 °C for 10–50 min in DES-water (0:1–4:6, *v/v*) containing chlorite salts (0–30.0 g/L), the autoclave

was quenched in an ice-water bath to room temperature. FAL yields were calculated as below equation:

$$\text{FAL yield (\%)} = \frac{\text{FAL produced (g)}}{\text{D-Xylose (g)}} \times \frac{150}{96} \times 100$$

3.5. Reuse of $\text{SO}_4^{2-}/\text{SnO}_2\text{-FFS}$ and DES

To evaluate the activity and stability of solid acid, $\text{SO}_4^{2-}/\text{SnO}_2\text{-FFS}$ was recovered and repeatedly reused five times to catalyze *D*-xylose into FAL. After each use, $\text{SO}_4^{2-}/\text{SnO}_2\text{-FFS}$ was extracted by suction flask, washed thoroughly with deionized water, and dried in an oven (60 °C). Then it was calcined in the muffle furnace to remove product residues and further sulfonation. The recovered $\text{SO}_4^{2-}/\text{SnO}_2\text{-FFS}$ was used in the next batch of reaction to measure its effect. Each batch was performed for 15 min in an autoclave (170 °C) containing 40 mL of DES–water (10:90, *v/v*), 20.0 g/L of *D*-xylose, and 20.0 g/L of ZnCl_2 . Subsequently, the reaction media were extracted with ethyl acetate three times, and the reaction liquid was reused five times.

3.6. Analytical Methods

Through FTIR, XRD, and BET and XPS [69], the diversity between $\text{SO}_4^{2-}/\text{SnO}_2\text{-FFS}$ and FFS was discovered. FAL was measured with HPLC as reported in reference [45]. $\text{NH}_3\text{-TPD}$ was carried out by using a ChemiSorb 2720 chemisorption system (Micromeritics, Norcross, GA, USA) to measure the acid strength of $\text{SO}_4^{2-}/\text{SnO}_2\text{-FFS}$. $\text{SO}_4^{2-}/\text{SnO}_2\text{-FFS}$ (0.10 g) was treated for 120 min with helium (300 °C). After the NH_3 adsorption for 60 min at 50 °C, $\text{SO}_4^{2-}/\text{SnO}_2\text{-FFS}$ was pretreated with helium to remove excessive NH_3 until a stable baseline was obtained. $\text{SO}_4^{2-}/\text{SnO}_2\text{-FFS}$ was heated to 850 °C for NH_3 desorption at a flow rate of 30–50 mL per minute and a heating rate of 10 °C per minute.

4. Conclusions

In this work, the abundant biobased FFS was used as a carrier to prepare the biochar $\text{SO}_4^{2-}/\text{SnO}_2\text{-FFS}$ catalyst. After the acid hydrolysis of corncob, xylose-rich corncob-hydrolysate was used as a substrate to produce FAL through the catalysis with biochar $\text{SO}_4^{2-}/\text{SnO}_2\text{-FFS}$ catalyst. In DES_{MLA} -water (DES_{MLA} , 10 vol%), the FAL yield was obtained at 70.5% by $\text{SO}_4^{2-}/\text{SnO}_2\text{-FFS}$ (3.6 wt.%) with ZnCl_2 (20.0 g/L) for 15 min under the temperature of 170 °C. The potential catalytic mechanism for the production of FAL from corncob catalyzed by $\text{SO}_4^{2-}/\text{SnO}_2\text{-FFS}$ in DES_{MLA} -water was proposed. An efficient method for the synthesis of biofuran from lignocellulose was successfully developed by using a biochar solid acid catalyst in a green reaction system.

Supplementary Materials: The following supporting information can be downloaded at: <https://www.mdpi.com/article/10.3390/catal13091277/s1>. Table S1. The FAL production from xylose catalyzed by FFS-based solid acids in DES_{MLA} -water (1/9, *v/v*) system.

Author Contributions: Methodology, software, validation, formal analysis, investigation, resources, data curation, writing—original draft preparation, L.Y., Y.L. and Y.W.; visualization, supervision, writing—review and editing, Y.H.; Methodology, formal analysis, investigation, resources, data curation, C.M. All authors have read and agreed to the published version of the manuscript.

Funding: This research was kindly funded by Open Project Program of the State Key Laboratory of Bioreactor Engineering.

Data Availability Statement: Not applicable.

Acknowledgments: The authors thank the Analysis and Testing Center (Changzhou University) for the analysis of solid acid with FT-IR, SEM, XRD, BET analysis, $\text{NH}_3\text{-TPD}$, and XPS.

Conflicts of Interest: The authors declare no conflict of interest.

Abbreviations

DES	deep eutectic solvent
LB	lignocellulosic biomass
FFS	fresh fish scale
L	Lewis
B	Brønsted
ChCl	choline chloride
CC	corn cob
HAP	hydroxyapatite
MA	malic acid
MLA	maleic acid
LA	lactic acid
CA	citric acid
TA	tartaric acid
HBD	hydrogen bond donor
XPS	X-ray photoelectron spectroscopy
HPLC	high performance liquid chromatography
FAL	furfural
FOL	furfuryl alcohol
XRD	X-ray diffraction
BET	Brunner–Emmet–Teller measurements
TG	thermogravimetric analysis
SEM	scanning electron microscopy
FT-IR	Fourier transform infrared spectroscopy

References

1. Chen, X.J.; Guo, T.; Mo, X.; Zhang, L.D.; Wang, R.F.; Xue, Y.N.; Fan, X.L.; Sun, S.L. Reduced nutrient release and greenhouse gas emissions of lignin-based coated urea by synergy of carbon black and polysiloxane. *Int. J. Biol. Macromol.* **2023**, *231*, 123334. [[CrossRef](#)]
2. He, Y.C.; Liu, F.; Di, J.H.; Ding, Y.; Zhu, Z.Z.; Wu, Y.Q.; Chen, L.; Wang, C.; Xue, Y.F.; Chong, G.G. Effective enzymatic saccharification of dilute NaOH extraction of chestnut shell pretreated by acidified aqueous ethylene glycol media. *Ind. Crops Prod.* **2016**, *81*, 129–138. [[CrossRef](#)]
3. Hu, L.; Wu, Z.; Jiang, Y.T.; Wang, X.Y.; He, A.Y.; Song, J.; Xu, J.M.; Zhou, S.Y.; Zhao, Y.J.; Xu, J.X. Recent advances in catalytic and autocatalytic production of biomass-derived 5-hydroxymethylfurfural. *Renew. Sustain. Energy Rev.* **2020**, *134*, 110317. [[CrossRef](#)]
4. Chen, X.J.; Guo, T.; Yang, H.C.; Zhang, L.D.; Xue, Y.N.; Wang, R.F.; Fan, X.L.; Sun, S.L. Environmentally friendly preparation of lignin/paraffin/epoxy resin composite-coated urea and evaluation for nitrogen efficiency in lettuce. *Int. J. Biol. Macromol.* **2022**, *221*, 1130–1141. [[CrossRef](#)]
5. Jia, W.; Zhang, J.; Yu, X.; Feng, Y.; Wang, Q.; Sun, Y.; Tang, X.; Zeng, X.; Lin, L. Insight into the Mars-van Krevelen mechanism for production 2,5-diformylfuran over FeN_x@C catalyst. *Biomass Bioenergy* **2022**, *156*, 106320. [[CrossRef](#)]
6. He, J.; Huang, C.; Lai, C.; Wang, Z.; Yuan, L.; Ragauskas, A.; Yan, Y.; Yong, Q. Revealing the mechanism of lignin re-polymerization inhibitor in acidic pretreatment and its impact on enzymatic hydrolysis. *Ind. Crops Prod.* **2022**, *179*, 114631. [[CrossRef](#)]
7. Hu, L.; Jiang, Y.; Wu, Z.; Wang, X.Y.; He, A.Y.; Xu, J.X.; Xu, J.M. State-of-the-art advances and perspectives in the separation of biomass-derived 5-hydroxymethylfurfural. *J. Clean. Prod.* **2020**, *276*, 124219. [[CrossRef](#)]
8. Ma, S.; Chen, B.; Zeng, A.; Li, Z.; Tang, X.; Sun, Y.; Lin, L.; Zeng, X. Chemical structure change of lignin extracted from bamboo biomass by maleic acid. *Int. J. Biol. Macromol.* **2022**, *221*, 986–993. [[CrossRef](#)] [[PubMed](#)]
9. Amini, E.; Valls, C.; Roncero, M.B. Ionic liquid-assisted bioconversion of lignocellulosic biomass for the development of value-added products. *J. Clean. Prod.* **2021**, *326*, 129275. [[CrossRef](#)]
10. Zhou, Z.; Ju, X.; Zhou, M.; Xu, X.; Fu, J.; Li, L. An enhanced ionic liquid-tolerant immobilized cellulase system via hydrogel microsphere for improving in situ saccharification of biomass. *Bioresour. Technol.* **2019**, *294*, 122146. [[CrossRef](#)]
11. Li, Q.; Ma, C.L.; Zhang, P.Q.; Li, Y.Y.; Zhu, X.; He, Y.C. Effective conversion of sugarcane bagasse to furfural by coconut shell activated carbon-based solid acid for enhancing whole-cell biosynthesis of furfurylamine. *Ind. Crops Prod.* **2021**, *160*, 113169. [[CrossRef](#)]
12. Ramírez, E.; Bringué, R.; Fité, C.; Iborra, M.; Tejero, J.; Cunill, F. Role of ion-exchange resins as catalyst in the reaction-network of transformation of biomass into biofuels. *J. Chem. Technol. Biotechnol.* **2017**, *92*, 2775–2786. [[CrossRef](#)]
13. Xia, Z.-H.; Zong, M.-H.; Li, N. Catalytic synthesis of 2,5-bis(hydroxymethyl)furan from 5-hydroxymethylfurfural by recombinant *Saccharomyces cerevisiae*. *Enzym. Microb. Technol.* **2020**, *134*, 109491. [[CrossRef](#)] [[PubMed](#)]

14. Yemiş, O.; Mazza, G. Acid-catalyzed conversion of xylose, xylan and straw into furfural by microwave-assisted reaction. *Bioresour. Technol.* **2011**, *102*, 7371–7378. [[CrossRef](#)]
15. Mittal, A.; Pilath, H.M.; Johnson, D.K. Direct conversion of biomass carbohydrates to platform chemicals: 5-hydroxymethylfurfural (HMF) and furfural. *Energy Fuels* **2020**, *34*, 3284–3293. [[CrossRef](#)]
16. Li, Y.Y.; Li, Q.; Zhang, P.Q.; Ma, C.L.; Xu, J.H.; He, Y.C. Catalytic conversion of corncob to furfuryl alcohol in tandem reaction with tin-loaded sulfonated zeolite and NADPH-dependent reductase biocatalyst. *Bioresour. Technol.* **2021**, *320*, 124267. [[CrossRef](#)] [[PubMed](#)]
17. Chatterjee, A.; Hu, X.; Lam, F.L.Y. Modified coal fly ash waste as an efficient heterogeneous catalyst for dehydration of xylose to furfural in biphasic medium. *Fuel* **2019**, *239*, 726–736. [[CrossRef](#)]
18. Chen, X.; Li, Z.; Zhang, L.; Wang, H.; Qiu, C.; Fan, X.; Sun, S. Preparation of a novel lignin-based film with high solid content and its physicochemical characteristics. *Ind. Crops Prod.* **2021**, *164*, 113396. [[CrossRef](#)]
19. Ji, L.; Tang, Z.; Yang, D.; Ma, C.; He, Y.C. Improved one-pot synthesis of furfural from corn stalk with heterogeneous catalysis using corn stalk as biobased carrier in deep eutectic solvent–water system. *Bioresour. Technol.* **2021**, *340*, 125691. [[CrossRef](#)]
20. Yang, Q.; Tang, Z.; Xiong, J.; He, Y. Sustainable chemoenzymatic cascade transformation of corncob to furfuryl alcohol with rice husk-based heterogeneous catalyst UST-Sn-RH. *Catalysts* **2022**, *13*, 37. [[CrossRef](#)]
21. Dulie, N.W.; Woldeyes, B.; Demsash, H.D. Synthesis of lignin-carbohydrate complex-based catalyst from *Eragrostis tef* straw and its catalytic performance in xylose dehydration to furfural. *Int. J. Biol. Macromol.* **2021**, *171*, 10–16. [[CrossRef](#)] [[PubMed](#)]
22. Zhang, T.; Li, W.; Xu, Z.; Liu, Q.; Ma, Q.; Jameel, H.; Chang, H.-M.; Ma, L. Catalytic conversion of xylose and corn stalk into furfural over carbon solid acid catalyst in γ -valerolactone. *Bioresour. Technol.* **2016**, *209*, 108–114. [[CrossRef](#)] [[PubMed](#)]
23. Xu, D.; Tang, W.; Tang, Z.; He, Y. An Efficient Strategy for Chemoenzymatic Conversion of Corn Stover to Furfuryl Alcohol in Deep Eutectic Solvent ChCl: PEG10000–Water Medium. *Catalysts* **2023**, *13*, 467. [[CrossRef](#)]
24. Smith, E.L.; Abbott, A.P.; Ryder, K.S. Deep eutectic solvents (DESs) and their applications. *Chem. Rev.* **2014**, *114*, 11060–11082. [[CrossRef](#)]
25. Zuo, M.; Wang, X.; Jia, W.; Zhu, Y.; Zeng, X.; Lin, L. Efficient 5-hydroxymethylfurfural synthesis from carbohydrates and food wastes in aqueous-natural deep eutectic solvent (A-NADES) with robust Al_2O_3 or $\text{Al}(\text{OH})_3$. *Fuel* **2022**, *369*, 125062. [[CrossRef](#)]
26. Li, A.L.; Hou, X.D.; Lin, K.P.; Zhang, X.; Fu, M.H. Rice straw pretreatment using deep eutectic solvents with different constituents molar ratios: Biomass fractionation, polysaccharides enzymatic digestion and solvent reuse. *J. Biosci. Bioeng.* **2018**, *126*, 346–354. [[CrossRef](#)]
27. Bu, C.Y.; Yan, Y.X.; Zou, L.H.; Ouyang, S.P.; Zheng, Z.J.; Ouyang, J. Comprehensive utilization of corncob for furfuryl alcohol production by chemo-enzymatic sequential catalysis in a biphasic system. *Bioresour. Technol.* **2021**, *319*, 124156. [[CrossRef](#)]
28. Yong, K.J.; Wu, T.Y.; Lee, C.B.T.L.; Lee, Z.J.; Liu, Q.; Jahim, J.M.; Zhou, Q.; Zhang, L. Furfural production from biomass residues: Current technologies, challenges and future prospects. *Biomass Bioenergy* **2022**, *161*, 106458. [[CrossRef](#)]
29. Mukkanti, V.B.; Tembhurkar, A.R. Defluoridation of water using adsorbent derived from the *Labeo rohita* (rohu) fish scales waste: Optimization, isotherms, kinetics, and thermodynamic study. *Sustain. Chem. Pharm.* **2021**, *23*, 100520. [[CrossRef](#)]
30. Qin, D.; Bi, S.; You, X.; Wang, M.; Cong, X.; Yuan, C.; Yu, M.; Cheng, X.; Chen, X.-G. Development and application of fish scale wastes as versatile natural biomaterials. *Chem. Eng. J.* **2022**, *428*, 131102. [[CrossRef](#)]
31. Yao, Q.F.; Zhou, D.S.; Yang, J.H.; Huang, W.T. Directly reusing waste fish scales for facile, large-scale and green extraction of fluorescent carbon nanoparticles and their application in sensing of ferric ions. *Sustain. Chem. Pharm.* **2020**, *17*, 100305. [[CrossRef](#)]
32. Tang, Z.; Li, Q.; Di, J.; Ma, C.; He, Y.-C. An efficient chemoenzymatic cascade strategy for transforming biomass into furfurylamine with lobster shell-based chemocatalyst and mutated ω -transaminase biocatalyst in methyl isobutyl ketone-water. *Bioresour. Technol.* **2023**, *369*, 128424. [[CrossRef](#)] [[PubMed](#)]
33. Romo, J.E.; Bollar, N.V.; Zimmermann, C.J.; Wettstein, S.G. Conversion of sugars and biomass to furans using heterogeneous catalysts in biphasic solvent systems. *ChemCatChem* **2018**, *10*, 4805–4816. [[CrossRef](#)] [[PubMed](#)]
34. Bhaumik, R.; Mondal, N.K.; Chatteraj, S. An optimization study for defluoridation from synthetic fluoride solution using scale of Indian major carp Catla (*Catla catla*): An unconventional biosorbent. *J. Fluor. Chem.* **2017**, *195*, 57–69. [[CrossRef](#)]
35. Ramadoss, P.; Arul, K.T.; Ramya, J.R.; Begam, M.R.; Chandra, V.S.; Manikandan, E. Enhanced mechanical strength and sustained drug release of gelatin/keratin scaffolds. *Mater. Lett.* **2017**, *186*, 109–112. [[CrossRef](#)]
36. George, A.M.; Tembhurkar, A.R. Analysis of equilibrium, kinetic, and thermodynamic parameters for biosorption of fluoride from water onto coconut (*Cocos nucifera* Linn.) root developed adsorbent. *Chin. J. Chem. Eng.* **2019**, *27*, 92–99. [[CrossRef](#)]
37. Kim, H.; Yang, S.; Kim, D.H. One-pot conversion of alginic acid into furfural using Amberlyst-15 as a solid acid catalyst in γ -butyrolactone/water co-solvent system. *Environ. Res.* **2020**, *187*, 109667. [[CrossRef](#)]
38. Xia, D.; Liu, Y.; Cheng, X.; Gu, P.; Chen, Q.; Zhang, Z. Temperature-tuned fish-scale biochar with two-dimensional homogeneous porous structure: A promising uranium extractant. *Appl. Surf. Sci.* **2022**, *591*, 153136. [[CrossRef](#)]
39. Zhang, W.; Sun, M.; Yin, J.; Lu, K.; Schwingenschlöggl, U.; Qiu, X.; Alshareef, H.N. Accordion-like carbon with high nitrogen doping for fast and stable K ion storage. *Adv. Energy Mater.* **2021**, *11*, 2101928. [[CrossRef](#)]
40. Ferrairo, B.M.; Mosquim, V.; de Azevedo-Silva, L.J.; Pires, L.A.; Padovini, D.S.S.; Magdalena, A.G.; Fortulan, C.A.; Lisboa-Filho, P.N.; Rubo, J.H.; Borges, A.F.S. Production of bovine hydroxyapatite nanoparticles as a promising biomaterial via mechanochemical and sonochemical methods. *Mater. Chem. Phys.* **2023**, *295*, 127046. [[CrossRef](#)]

41. Teng, X.; Si, Z.; Li, S.; Yang, Y.; Wang, Z.; Li, G.; Zhao, J.; Cai, D.; Qin, P. Tin-loaded sulfonated rape pollen for efficient catalytic production of furfural from corn stover. *Ind. Crops Prod.* **2020**, *151*, 112481. [[CrossRef](#)]
42. Piccirillo, C.; Pullar, R.C.; Tobaldi, D.M.; Castro, P.M.L.; Pintado, M.M.E. Hydroxyapatite and chloroapatite derived from sardine by-products. *Ceram. Int.* **2014**, *40*, 13231–13240. [[CrossRef](#)]
43. Jia, Q.; Teng, X.; Yu, S.; Si, Z.; Li, G.; Zhou, M.; Cai, D.; Qin, P.; Chen, B. Production of furfural from xylose and hemicelluloses using tin-loaded sulfonated diatomite as solid acid catalyst in biphasic system. *Bioresour. Technol. Rep.* **2019**, *6*, 145–151. [[CrossRef](#)]
44. Huang, Y.; Liao, X.; Deng, Y.; He, Y. Co-catalysis of corncob with dilute formic acid plus solid acid $\text{SO}_4^{2-}/\text{SnO}_2$ -montmorillonite under the microwave for enhancing the biosynthesis of furfuralcohol. *Catal. Commun.* **2019**, *120*, 38–41. [[CrossRef](#)]
45. Xue, X.X.; Ma, C.L.; Di, J.H.; Huo, X.Y.; He, Y.C. One-pot chemo-enzymatic conversion of *D*-xylose to furfuralcohol by sequential dehydration with oxalic acid plus tin-based solid acid and bioreduction with whole-cells. *Bioresour. Technol.* **2018**, *268*, 292–299. [[CrossRef](#)]
46. He, Y.C.; Jiang, C.X.; Chong, G.G.; Di, J.H.; Wu, Y.F.; Wang, B.Q.; Xue, X.X.; Ma, C.L. Chemical-enzymatic conversion of corncob-derived xylose to furfuralcohol by the tandem catalysis with $\text{SO}_4^{2-}/\text{SnO}_2$ -kaoline and *E. coli* CCZU-T15 cells in toluene-water media. *Bioresour. Technol.* **2017**, *245*, 841–849. [[CrossRef](#)]
47. Bhaumik, P.; Dhepe, P.L. Exceptionally high yields of furfural from assorted raw biomass over solid acids. *RSC Adv.* **2014**, *4*, 26215–26221. [[CrossRef](#)]
48. Hua, D.; Ding, H.; Liu, Y.; Li, J.; Han, B. Dehydration of xylose to furfural over imidazolium-based ionic liquid with phase separation. *Catalysts* **2021**, *11*, 1552. [[CrossRef](#)]
49. Fihri, A.; Len, C.; Varma, R.S.; Solhy, A. Hydroxyapatite: A review of syntheses, structure and applications in heterogeneous catalysis. *Coord. Chem. Rev.* **2017**, *347*, 48–76. [[CrossRef](#)]
50. Weingarten, R.; Tompsett, G.A.; Conner, W.C.; Huber, G.W. Design of solid acid catalysts for aqueous-phase dehydration of carbohydrates: The role of Lewis and Brønsted acid sites. *J. Catal.* **2011**, *279*, 174–182. [[CrossRef](#)]
51. Tang, X.; Zuo, M.; Li, Z.; Liu, H.; Xiong, C.; Zeng, X.; Sun, Y.; Hu, L.; Liu, S.; Lei, T.; et al. Green processing of lignocellulosic biomass and its derivatives in deep eutectic solvents. *ChemSusChem* **2017**, *10*, 2696–2706. [[CrossRef](#)]
52. Zhang, S.; Ma, C.; Li, Q.; Li, Q.; He, Y.C. Efficient chemoenzymatic valorization of biobased *D*-fructose into 2,5-bis(hydroxymethyl)furan with deep eutectic solvent Lactic acid:Betaine and *Pseudomonas putida* S12 whole cells. *Bioresour. Technol.* **2022**, *344*, 126299. [[CrossRef](#)] [[PubMed](#)]
53. Pan, L.; Li, Q.; Tao, Y.; Ma, C.; Chai, H.; Ai, Y.; He, Y.-C. An efficient chemoenzymatic strategy for valorisation of corncob to furfuryl alcohol in CA: Betaine-water. *Ind. Crops Prod.* **2022**, *186*, 115203. [[CrossRef](#)]
54. Shen, J.; Gao, R.; He, Y.-C.; Ma, C. Efficient synthesis of furfural from waste biomasses by sulfonated crab shell-based solid acid in a sustainable approach. *Ind. Crops Prod.* **2023**, *202*, 116989. [[CrossRef](#)]
55. Sadula, S.; Oesterling, O.; Nardone, A.; Dinkelacker, B.; Saha, B. One-pot integrated processing of biopolymers to furfurals in molten salt hydrate: Understanding synergy in acidity. *Green Chem.* **2017**, *19*, 3888–3898. [[CrossRef](#)]
56. Hu, B.; Xie, W.L.; Wu, Y.T.; Liu, J.; Ma, S.W.; Wang, T.P.; Zheng, S.; Lu, Q. Mechanism study on the formation of furfural during zinc chloride-catalyzed pyrolysis of xylose. *Fuel* **2021**, *295*, 120656. [[CrossRef](#)]
57. Yang, D.; Ma, C.; Peng, B.; Xu, J.; He, Y.C. Synthesis of furoic acid from biomass via tandem pretreatment and biocatalysis. *Ind. Crops Prod.* **2020**, *153*, 112580. [[CrossRef](#)]
58. Faruque, M.O.; Razzak, S.A.; Hossain, M.M. Application of heterogeneous catalysts for biodiesel production from microalgal oil—A review. *Catalysts* **2020**, *10*, 1025. [[CrossRef](#)]
59. Li, H.; Ren, J.; Zhong, L.; Sun, R.; Liang, L. Production of furfural from xylose, water-insoluble hemicelluloses and water-soluble fraction of corncob via a tin-loaded montmorillonite solid acid catalyst. *Bioresour. Technol.* **2015**, *176*, 242–248. [[CrossRef](#)]
60. Muhammad, N.; Gao, Y.; Iqbal, F.; Ahmad, P.; Ge, R.; Nishan, U.; Rahim, A.; Gonfa, G.; Ullah, Z. Extraction of biocompatible hydroxyapatite from fish scales using novel approach of ionic liquid pretreatment. *Sep. Purif. Technol.* **2016**, *161*, 129–135. [[CrossRef](#)]
61. Cai, D.; Chen, H.; Zhang, C.; Teng, X.; Li, X.; Si, Z.; Li, G.; Yang, S.; Wang, G.; Qin, P. Carbonized core-shell diatomite for efficient catalytic furfural production from corn cob. *J. Clean. Prod.* **2021**, *283*, 125410. [[CrossRef](#)]
62. Zhu, C.; Wang, K.; Luo, J.; Tian, B.; Sun, J.; Liu, X.; Zhu, W.; Zou, Z. Solid superacid $\text{SO}_4^{2-}-\text{S}_2\text{O}_8^{2-}/\text{SnO}_2-\text{Nd}_2\text{O}_3$ -catalyzed esterification of α -aromatic amino acids. *Mol. Catal.* **2023**, *535*, 112833. [[CrossRef](#)]
63. Ni, J.; Di, J.; Ma, C.; He, Y.C. Valorisation of corncob into furfuryl alcohol and furoic acid via chemoenzymatic cascade catalysis. *Bioresour. Bioprocess.* **2021**, *8*, 113. [[CrossRef](#)]
64. Enslow, K.R.; Bell, A.T. The role of metal halides in enhancing the dehydration of xylose to furfural. *ChemCatChem* **2015**, *7*, 479–489. [[CrossRef](#)]
65. Zha, J.; Fan, B.; He, J.; He, Y.-C.; Ma, C. Valorization of biomass to furfural by chestnut shell-based solid acid in methyl isobutyl ketone–water–sodium chloride system. *Appl. Biochem. Biotechnol.* **2022**, *194*, 2021–2035. [[CrossRef](#)]
66. Mujtaba, M.; Fernandes Fraceto, L.; Fazeli, M.; Mukherjee, S.; Savassa, S.M.; Araujo de Medeiros, G.; do Espírito Santo Pereira, A.; Mancini, S.D.; Lipponen, J.; Vilaplana, F. Lignocellulosic biomass from agricultural waste to the circular economy: A review with focus on biofuels, biocomposites and bioplastics. *J. Clean. Prod.* **2023**, *402*, 136815. [[CrossRef](#)]
67. Arevalo-Gallegos, A.; Ahmad, Z.; Asgher, M.; Parra-Saldivar, R.; Iqbal, H.M. Lignocellulose: A sustainable material to produce value-added products with a zero waste approach—A review. *Int. J. Biol. Macromol.* **2017**, *99*, 308–318. [[CrossRef](#)]

68. Singh, M.B.; Kumar, V.S.; Chaudhary, M.; Singh, P. A mini review on synthesis, properties and applications of deep eutectic solvents. *J. Indian Chem. Soc.* **2021**, *98*, 100210. [[CrossRef](#)]
69. Ni, J.; Li, Q.; Gong, L.; Liao, X.L.; Zhang, Z.J.; Ma, C.; He, Y. Highly efficient chemoenzymatic cascade catalysis of biomass into furfurylamine by a heterogeneous shrimp shell-based chemocatalyst and an ω -transaminase biocatalyst in deep eutectic solvent–water. *ACS Sustain. Chem. Eng.* **2021**, *9*, 13084–13095. [[CrossRef](#)]

Disclaimer/Publisher’s Note: The statements, opinions and data contained in all publications are solely those of the individual author(s) and contributor(s) and not of MDPI and/or the editor(s). MDPI and/or the editor(s) disclaim responsibility for any injury to people or property resulting from any ideas, methods, instructions or products referred to in the content.